Electronic Supplementary Information

Enhanced performance a-GaOx thin-film transistor photodetectors via in-situ

hydrogen incorporation using water vapor

Ming-Hang Lei[1,2], Jun-Yan Ren[1], Jing-Ting Sun[1], Hong-Yu Chen[1], Zhao-Xing Fu[1,2],

Zhi-Peng Chen[1,2], Ting-Ting Jin[1], Hui-Ze Tang[1], Liang Jing[3], Ling-Yan Liang[1*], and

Hong-Tao Cao[1,4*]

1. Laboratory of Atomic-scale and Micro & Nano Manufacturing, Ningbo Institute of

Materials Technology and Engineering, Chinese Academy of Sciences, Ningbo

315201, China.

2. Nano Science and Technology Institute, University of Science and Technology of

China, Suzhou 215123, China.

3. Metro Group Co., Ltd., Ningbo 315101, People's Republic of China.

4.Center of Materials Science and Optoelectronics Engineering, University of Chinese

Academy of Sciences, Beijing 100049, China.

*E-mail: lly@nimte.ac.cn (Lingyan Liang)

*E-mail: h_cao@nimte.ac.cn (Hongtao Cao)

8 pages, 5 figures, 1 table

Table of Contents:

Supplementary Note 1. Ga 2p$_{3/2}$ XPS spectra, including hydroxyl content variation with water flux ratio

The XPS analysis was performed on the Ga 2p$_{3/2}$ spectra of a-GaO$_x$ thin films. The results indicate that, for the as-deposited films, the incorporation of water vapor during sputtering induced a shift in the Ga 2p$_{3/2}$ binding energy from 1117.88 eV (W-0 sample) to 1117.82 eV (W-5 sample). In contrast, for the annealed films, the Ga 2p$_{3/2}$ binding energy shifted from 1117.67 eV (W-0 sample) to 1117.86 eV (W-3 sample). Changes in the Ga 2p$_{3/2}$ binding energy reflect the extent of oxidation of gallium atoms in a-GaO$_x$ films, which indirectly indicate variations in the oxygen vacancy concentration within the a-GaO$_x$ thin films. Additionally, we plotted the variation of the O$_{III}$ component of the annealed a-GaO$_x$ films to determine whether hydrogen is incorporated within the film in a form distinct from hydroxyl groups.
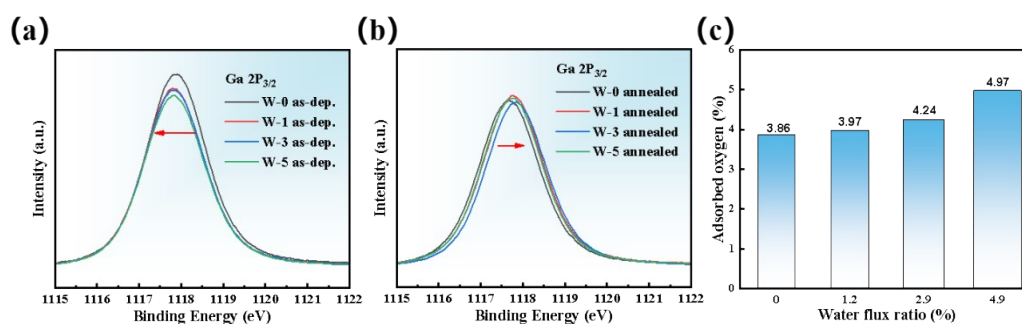

Figure S1. (a) Variation of Ga 2p$_{3/2}$ core level spectra of a-GaO$_x$ thin films in the as-deposited state, (b) Variation of Ga 2p$_{3/2}$ core level spectra of a-GaO$_x$ thin films in the annealed state, (c) the variation trend of hydroxyl with water flux ratio.

Supplementary Note 2. Optical property analysis of a-GaO$_x$ thin films in the as-deposited state, including bandgap, absorption spectrum, and refractive index

The optical properties of the as-deposited a-GaO$_x$ thin films were analyzed using variable-angle spectroscopic ellipsometry. The results indicate that, although the bandgap continues to broaden gradually upon water vapor incorporation, the refractive index decreases. This suggests a reduction in film density, which is consistent with the findings from XRR measurements, further confirming the impact of water vapor on the density of the as-deposited films.
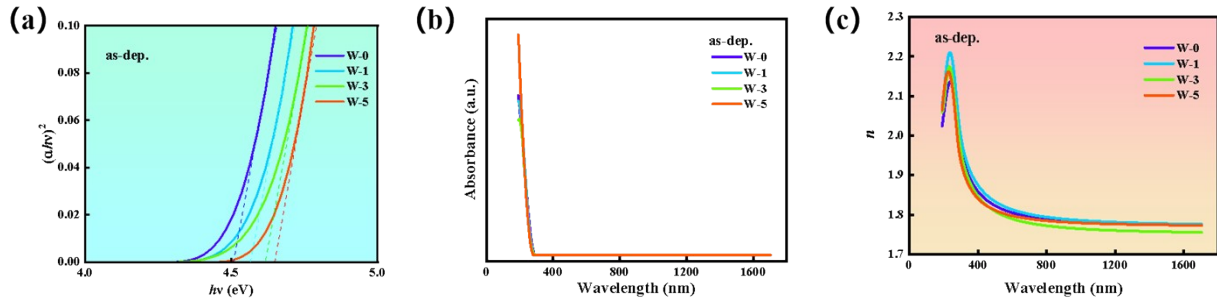

Figure S2. Optical property analysis of a-GaO$_x$ thin films in the as-deposited state under different water flux ratios: (a) Bandgap diagram, (b) Absorption spectrum, and (c) Refractive index.

Supplementary Note 3. Raw data and fitted curves for XRR test characterization

Figure S3 shows both the original experimental XRR data and the fitted curves obtained during the fitting process, and they have a high fitting accuracy. In a word, to ensure accuracy and reliability, the parameters reported in the main text, including mass density, were directly obtained from these fitted curves.
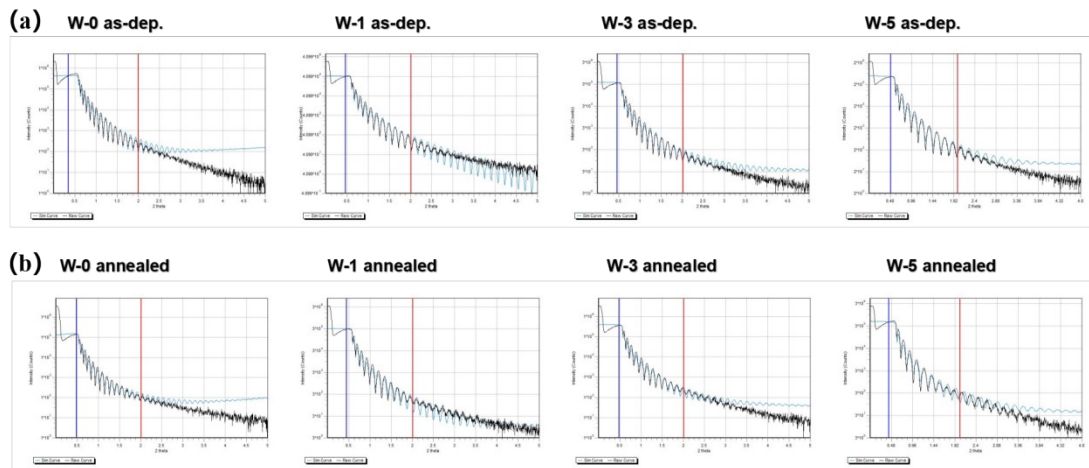

Figure S3. XRR analysis of a-GaO$_x$ films with different water flux ratios: (a) XRR raw data and fitted curves for four samples in the as-deposited state, (b) XRR raw data and fitted curves for four samples in the annealed state, the fitting range is selected between the blue and red lines.
.

Supplementary Note 4. Variation curves of responsivity with V_{GS} for a-GaO$_x$ thin film phototransistors under different wavelengths of illumination

We measured the transfer curves of a-GaOx TFT PDs under both illuminated and dark conditions and calculated the responsivity to evaluate its variation with gate voltage at different wavelengths. Additionally, we compared the overall trend of responsivity under different water flux conditions to assess the impact of water vapor incorporation on the optoelectronic performance of the devices.
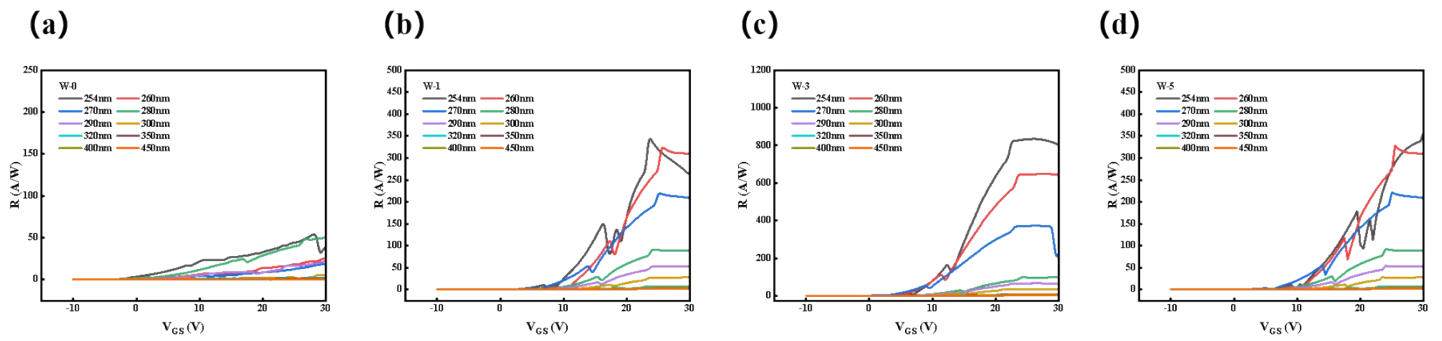
(a) **(b)** **(c)** **(d)**

Figure S4. Variation curves of responsivity with V_{GS} for a-GaO$_x$ thin film phototransistors under different wavelengths of illumination: (a) W-0, (b) W-1, (c) W-3, and (d) W-5.

Supplementary Note 5. Response recovery time of a-GaO$_x$ thin film phototransistors obtained using double e exponential fitting

we employed a double-exponential fitting method instead of directly calculating the response time from the 10%-90% current level change, as shown in Figure S4. Using this more accurate approach, we found that the response time of W-3 is only slightly longer than that of W-1, without a significant increase.
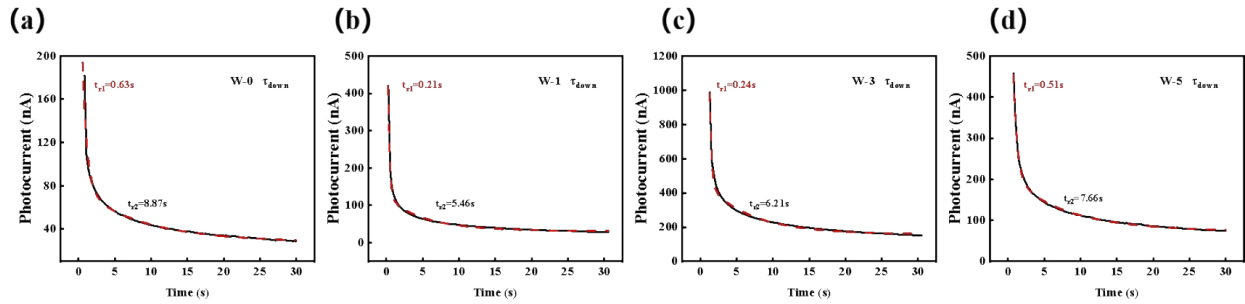

Figure S5. Response recovery time obtained using double e exponential fitting: (a) W-0, (b) W-1, (c) W-3, and (d) W-5.

Supplementary Note 6. UV/Visible rejection ratios for a-GaO$_x$ thin film phototransistors

To evaluate the UV/visible rejection capability of the a-GaOx TFT PDs, we calculated the rejection ratios at two representative visible wavelengths (400 nm and 450 nm) under different conditions. The UV/visible rejection ratios, represented as R$_{254}$/R$_{400}$ and R$_{254}$/R$_{450}$, quantify the ability of the devices to suppress interference from visible light while maintaining high responsivity in the UV spectrum.

Table S1   UV-Vis rejection ratio of different samples

Samples	R_{254} (A/W)	R_{400} (A/W)	R_{450} (A/W)	R_{254}/R_{400}	R_{254}/R_{450}
W-0	44.05	0.09574	0.02866	4.60×10^2	1.53×10^3
W-1	319.4	0.63936	0.28354	4.90×10^2	1.12×10^3
W-3	832.8	0.96542	0.53987	8.62×10^2	1.54×10^3
W-5	323.5	0.47751	0.63936	6.78×10^2	5.06×10^2